JOURNAL OF COMPUTATIONAL INNOVATION AND ANALYTICS
https://e-journal.uum.edu.my/index.php/jcia

How to cite this article:
Forooshani, M. E., Gegov, A., Pepin, N. & Adda, M. (2023). Creating air temperature models for high-elevation desert areas using machine learning. *Journal of Computational Innovation and Analytics, 2(1),* 1-19. https://doi.org/10.32890/jcia2023.2.1.1

CREATING AIR TEMPERATURE MODELS FOR HIGH-ELEVATION DESERT AREAS USING MACHINE LEARNING

[1]Massoud Forooshani, [2]Alexander Gegov,
[3]Nick Pepin & [4]Mo Adda
[1,2&4]School of Computing,
University of Portsmouth, United Kingdom
[2]English Language Faculty of Engineering,
Technical University of Sofia, Bulgaria
[3]School of the Environment, Geography and Geosciences,
University of Portsmouth, United Kingdom

[1]Corresponding author: massoud.forooshani@port.ac.uk

Received: 24/5/2022 Revised: 2/11/2022 Accepted: 16/11/2022 Published: 30/1/2023

ABSTRACT

The standard way to measure the air temperature (Ta) as the key variable in climate change studies is at 2m height above the surface at a fixed location (weather station). In contrast, the surface temperature (Ts) can be measured by satellites over large areas. Estimation of Ta from Ts is one potential way of overcoming shortages due to uneven or irregular distributions of weather stations. However, whether this is successful has not been assessed in high-elevation regions. This is particularly important in high-elevation regions. In this study, we estimate Ta in the high-elevation desert zone of Kilimanjaro (>4500m) using four models (five models including the benchmark model) with

unique sets of inputs using five machine learning (ML) algorithms. Note that different combinations of Ta and Ts were tested as inputs to evaluate the potential of Ts as a proxy for Ta. The Root Mean Square Error (RMSE) for each model was compared with a benchmark model and ranked according to their RMSE. Similarly, models and algorithms were ranked in terms of reliability and consistency. Correspondingly, results were compared with the benchmark model. Three models out of four outperformed the benchmark model in the consistency ranking, while two out of four models outperformed the benchmark model in the reliability ranking. Therefore, ML algorithms are efficient tools for estimating Ta from Ts in this high-elevation desert environment. However, models using Ts only as inputs were not as accurate as models that used Ta from an earlier time period as one of the inputs. This highlights the amount of de-coupling between Ta and TS at high elevations, which provides a challenge for using Ts alone as a proxy for Ta in this zone.

Keywords: Air temperature, desert, Kilimanjaro, machine learning, surface temperature.

INTRODUCTION

Ta is a key variable in climate change measurements (Pepin et al., 2019; Benali et al., 2012; Vancutsem et al., 2010), and much research has suggested that mountain regions may be warming faster than lower elevations. This phenomenon is called Elevation Dependent Warming (EDW) (Pepin et al., 2019; Palazzi et al., 2019). However, there are limitations associated with Ta measurements made at weather stations. The fixed locations of available measurements limit validity to the precise location, contrasting with climate change studies that need information representative of large areas. Many mountain regions are not easily accessible. Hence, weather stations cannot be maintained everywhere, leading to an uneven distribution of stations in mountains and an underrepresentation of stations at high elevations (Pepin et al., 2019; Palazzi et al., 2019). Changes in instrument exposure, the lack of long time series, and gaps in records at all stations are some of the other problems with weather station data, which is not always available and has limited temporal and spatial coverage. Contrarily, satellites can measure the Earth's Ts globally, and data is nearly always available and has extensive spatial coverage. Thus, Ts can be used to estimate Ta (Pepin et al., 2016; Urban et al., 2013; Hachem et al., 2012; Shen & Leptoukh, 2011).

In this study, we utilize the example of Kilimanjaro as a test bed for examining the extent to which Ts can be used to estimate Ta. There are several weather stations installed in a transect across the mountain. Kilimanjaro is the largest and highest free-standing mountain in the world. It is located near the equator. Its base lies below 1000m above sea level, and its peak rises to 5895m. The mountain is divided into several vegetation/elevation zones. The approximate elevations of the zones include urban and agricultural (1000 – 1800m), forest (1800 – 3000m), heather (3100 – 3900m), moorland (3900 – 4500m), high elevation desert (4500 – 5800m) and a small ice cap (>5500m). The desert zone starts around 4500m, extends to the ice cap, and is one of the highest-elevation deserts in the world. It has very little vegetation, is dry, and the temperature regime is dominated by solar radiation since there is little cloud cover (Pepin et al., 2016).

Some of the ecosystems on Kilimanjaro have been the subject of research because of their high impact on regional and local climate change. This is the case for the rainforest, a critical water resource for the lower slopes (Hemp, 2009; Hemp, 2005). The summit ice cap has also been of intense interest because it is experiencing a rapid decline (Mote & Kaser, 2007; Mölg et al., 2003; Thompson et al., 2002). In general, the Kilimanjaro desert zone has been much less studied, and the perceived lack of impact on climate change has led to a gap in the literature about this high-elevation desert. In the context of Ts measurements, it can provide a unique baseline to be compared with other surface types as it is the only surface not covered by vegetation (or ice), and it reflects the true impact of intense solar radiation coupled with low air pressure (500-700 mb) at high elevation.

The differences between Ta and Ts are particularly stark in the desert zone. Ts are highly dependent on the surface type and change rapidly in space and time as the surface heats and cools in response to solar radiation. Other than that, the Ta demonstrates more stability in time and space and, although measured at a fixed point, could be argued to be more representative of the temperature over a slightly wider area. The relationship between the two variables is non-linear and complex. The application of ML algorithms, with their power in modeling non-linear and complex systems, is a promising option compared to other statistical methods. We apply this approach in this study. The next sections will cover past studies, methodology, data collection, data analysis, results, and conclusions.

The research problems and solutions can be summarized as follows:

- Weather stations data (Ta): The fixed locations of weather stations limit the validity of Ta measurements to the precise location, uneven distribution of stations in mountains, under-representation of stations at high elevations, Changes in instrument exposure times, the lack of long time series, gaps in records at all stations,
- Satellite data (Ts): is nearly always available and has extensive spatial and temporal coverage.
- Climate change: needs information representative of large areas over long periods of time.
- The relationship between Ta and Ts: is non-linear and complex.
- ML algorithms are powerful tools for modeling non-linear and complex systems.

PAST STUDIES

Modeling Ts from Ta

There have been many attempts to derive Ta from the Ts in different environments. These include Urban et al. (2013) in the Arctic, Hachem et al. (2012) in Canada and Alaska, Shen & Leptoukh (2011) in Russia and China, Pepin et al. (2019) and Xu et al. (2018) on the Tibetan Plateau in western China, Benali et al. (2012) in Portugal, while Pepin et al. (2016) and Vancutsem et al. (2010) in Africa. Note that Potter & Coppernoll-Houston (2019), Colombi et al. (2007), and Zhou & Wang (2016) provide the most recent studies on the land Ts in deserts.

Not all of these have specifically focused on high mountain environments where the difference between Ta and Ts can become instantaneously large due to intense radiation and low air pressure at high elevations. They also cover a wide range of different vegetation zones.

In all cases, it is common to build regression models to estimate Ta from Ts. Although regression models are a solid framework for modeling and have been widely applied in the references above, the introduction of new ML algorithms to the research environment in recent years presents an alternative approach that needs to be evaluated.

Machine Learning

The application of ML algorithms in climate science and weather forecasting goes back to the works of Moninger et al. (1987) and McCann (1992), who investigated the application of Expert Systems (ES) and Artificial Neural Networks (ANN), respectively.

ML has also been applied to the prediction of Ta from Ts but in a limited way. The research papers (Kumari et al., 2012; Zhao et al., 2007; Hayati & Mohebi, 2007; Jang et al., 2004; Schizas et al., 1991) all utilize ANN for this purpose. However, other ML algorithms, including Adaptive Neuro-Fuzzy Inference Systems (ANFIS), have been restricted to weather forecasting applications and have not been used to estimate Ta from the Ts in a climate context. Furthermore, these past research examples commonly employed variable types other than Ta and Ts to estimate Ta. Therefore, for the first time, our work uses a combination of a wide variety of ML algorithms with the core Ta and Ts variables to present a simple but efficient approach to estimating Ta from the Ts in a high-elevation desert environment.

Past research on the application of ML algorithms in the estimation of Ta is limited to a few algorithms. Moreover, it has not been applied in a high-elevation context. Hence, this research will evaluate the application of several ML algorithms using only the two core variables, namely Ts and Ta, to present a novel and simple but efficient approach to estimating Ta from Ts.

RESEARCH METHODOLOGY

Modeling large-scale, complex, non-linear, ill-defined, and uncertain systems such as climate change systems have been a prime concern for a long time. The application of ML algorithms, such as fuzzy systems and neural networks, has opened a path for more ML algorithms to be tested and used in this field. Five main algorithms were employed in this study (described below).

ANFIS (Adaptive Neuro Fuzzy System)

ANFIS is an implementation of a Fuzzy Inference System (FIS) on top of the architecture of an ANN, combining the power of a fuzzy rule base with the learning capability of neural networks. For a discussion, see (Jang, 1993).

Figure 1

ANFIS Architecture (Bonissone, n.d.)

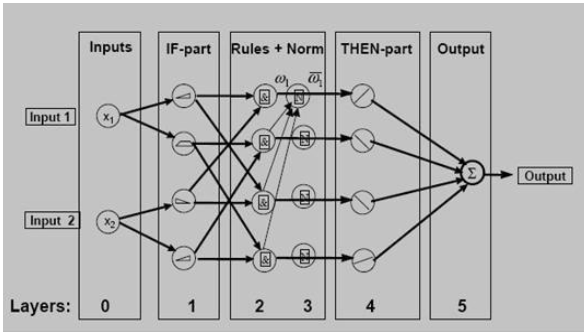

Linear Regression

Linear regression is the modeling of the relationship between one or more linear independent variables to predict a dependent variable. The basic regression model for one independent variable is in the form of Equation 1 (Neter et al., 1996).

$$y_i = \beta_0 + \beta_1 + X_i + \epsilon_i, \quad (1)$$

•where y_i is the response variable in the i^{th} trial
• β_0 and β_1 are parameters
• X_i is a known constant (the value of the independent variable in the i^{th} trial)
• ϵ_i is a random error
• β_0 and β_1 are called regression coefficients.
•β_1 is the slope of the regression line.
•β_0 is the Y-intercept of the regression line.

Polynomial Regression

Polynomial multiple regression models are special cases of general linear regression models with more than one independent variable, and variables can take various powers. The general form for one independent variable in second order is in Equation 2 (Neter et al., 1996).

$$FWER = Pr(V > 0). \quad (2)$$

Support Vector Machine (SVM)

Support vector machine (SVM) is one of the most popular ML algorithms, developed by (Cortes & Vapnik, 1995). It was packaged

as a LIBSVM library by Lin & Chang (2001) to make the application easier. Note that SVM maps the input vectors into a high dimensional feature space Z through non-linear mapping chosen a priori. In this space, a linear decision surface is constructed with special properties that ensure the high generalization ability of the network.

Figure 2

Support Vector Machine (Shehzadex, 2021)

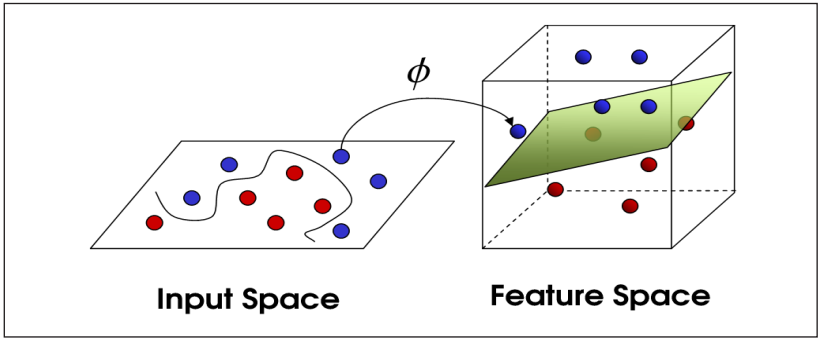

Simple Regression Tree

Regression trees are a type of decision tree that targets continuous variables. This algorithm builds a tree to predict the output from various inputs in the recursive partitioning mode. The space is continuously divided into smaller areas containing a simple model. Other than that, the global model has two parts, the recursive partitioning, and the simple model. The regression tree uses a tree to represent the recursive partitioning in which each cell or terminal node contains a simple model. The model in each node is a constant estimate of the output.

If the points $(X_1, Y_1), (X_2, Y_2), \ldots (X_c, Y_c)$ are all the samples belonging to the leaf node I. Subsequently, the model for l as in Equation 3 (Brieman et al., 1984).

$$\hat{y} = \frac{1}{C}\sum_{i=1}^{c} y_i. \tag{3}$$

DATA COLLECTION AND ANALYSIS

Data

The full data set consists of Ta and Ts recorded at 22 sites across Kilimanjaro between 990 and 5803m above sea level (Pepin, 2004).

It has been applied before by Pepin et al. (2016) in a preliminary comparison of Ta and Ts across the mountain. In this study, five stations within the desert zone were selected. Two stations are located on the east, two on the southwest, and one on the mountain's northwest side. The range of elevations of the chosen stations is from 4966 to 5794m.

The Ta at each site is recorded using automatic data loggers (Hobo U23-001) installed in a radiation shield at 2m above ground level. Observations were recorded as an instantaneous value every 30 minutes. The Ts are retrieved from the Terra satellite and consist of the MODIS product MOD11A2, which provides an 8-day mean Ts at 1km by 1km resolution. The mean time of the satellite overpasses is 1030 local solar time (day) and 2230 local solar time (night).

For a direct comparison with Ts, the mean Ta taken at 1030 and 2230 East African Time (EAT) were averaged over the same 8-day periods as the Ts. All 8 days were utilized for comparison.

Variables Used in Machine Learning Models

Five variables were defined, four of which represented day (1030) and night (2230) Ta and Ts. The novel variable ΔTs was defined as the difference between day and night Ts (and is a proxy for solar radiation). Four variables were used as input, and one variable was used as output (TaD).

Table 1

List of Five Variables

Variable	Input/output	Description
TaD	Output	Air temperature of the day
TaN		Air temperature of the night
TsD		Surface temperature of the day
TsN	Inputs	Surface temperature of the night
ΔTs		Solar Radiation (TsD - TsN)

Models

Using a benchmark model in ML is a standard way of evaluating/comparing the performance of novel models with an accepted standard. The benchmark model is applied to our research data, and

results are compared with the results from the novel models. Other than that, the benchmark model simulation was based on research presented by Kumar (2012), in which ANFIS was employed to predict Ta as input and output. The benchmark simulation used TaN as input and TaD as output.

The scope of this research is limited to the estimation of Ta from Ts. This approach's power is based on the application of ML algorithms to keep inputs at a minimum. Using ΔTs as a proxy for solar radiation is one way of avoiding using extra variables. Other variables such as solar radiation, TVX, humidity, elevation, and pressure are used by other researchers widely.

Four different sets of inputs as four novel models were evaluated to estimate daytime, Ta. Different combinations of these variables each have a meaning in the context of climate change studies (see Tables 1 and 2).

Table 2

Models

Model	Acronym	Inputs	Output
Model-1	m1	TsN, TaN, TsD	TaD
Model-2	m2	TsN, TsD	TaD
Model-3	m3	TaN, ΔTs	TaD
Model-4	m4	ΔTs	TaD
Benchmark model	bm	TaN	TaD

K-fold Cross Validation

The selection of 4-fold cross-validation as a performance metric was based on the minimum of data rows available for one-fold.

Data Sets

To avoid the confusion caused by different naming conventions for data sets applied by authors, the following naming conventions and descriptions were adopted from MATLAB software:

- The testing data set contained 20% of the main data set, and its objective was to test the generalizability of the trained and cross-validated model with unseen data.

- The learning data set contained 80% of the main data set from which the training (75%) and checking (25%) data sets were selected for 4-fold cross-validation to prevent overfitting of the model. The average RMSE was calculated and used as the main performance metric for each model.

Data Pre-processing

Requirements that determined the data per-processing include:

- Two software platforms were used for data pre-processing, MATLAB (ANFIS GUI) version R2020a (2020) and KNIME Analytics Platform Version 4.3.4 (2020). Note that MATLAB needed a special data preparation process, whereas KNIME used the same data files prepared for MATLAB.
- The ML analysis stages of training, checking, and testing needed different data sets prepared for each stage.
- K-fold cross-validation: 4-fold cross-validation selected regarding the minimum number of data rows needed for each fold. Data needed to be prepared for each fold individually.
- Variables need to be extracted from the main data files.
- Novel models with different inputs needed separate data sets.

SIMULATION RESULTS

The Models RMSE

Table 3 contains the RMSE (between observed and predicted Ta) for the four novel models (m1-m4) and the benchmark model (bm) using each of the five algorithms. Figures are the average RMSE of the 4-fold cross-validation. The RMSE unit is Celsius degrees and should be interpreted in the context of the climate change studies in which ‘’ errors generally fall in the 2–3°C range while the level of precision generally considered as accurate is 1–2°C (Benali et al., 2012). Therefore, these accuracy ranges were regarded in interpreting the results.

Models m1, m3, and bm (benchmark) model’s RMSE fall between 2-3°C, which is in the accepted accuracy range. Meanwhile, models m2 and m4 fall well out of the accuracy range. Both models include Ts as their input, meaning the Ts as the sole input cannot be used to estimate Ta well in the desert zone. Models m1 and m3 tend to be fairly similar, and RMSE is usually between 2 and 3°C (greyed).

Table 3

Models RMSE

Models	Inputs	ANFIS	Polynomial regression	Linear regression	LIBSVM	Simple regression tree	Average RMSE
m1	TsN, TaN, TsD	2.152625	2.138	2.156	2.424	2.342	2.242525
m2	TsN, TsD	8.0931	7.67	7.667	9.82	10.283	8.70662
m3	TaN, ΔTs	2.029875	2.112	2.157	2.204	2.621	2.224775
m4	ΔTs	8.231325	8.183	8.299	9.153	11.21	9.015265
bm	TaN	2.08415	2.195	2.278	2.349	2.533	2.28783
Average RMSE		4.518215	4.4596	4.5114	5.19	5.7978	-

The Best Model

The best model in Table 3 is m3 combined with the ANFIS algorithm. This model gained the average (4-folds) RMSE = 2.029875, an acceptable accuracy range. However, the 3-fold of this model came up with the RMSE= 2.0076, which is on the edge of the ideal accuracy range (1 – 2°C). Note that testing data in Figure 3 is presented with blue dots, whereas the FIS output is presented with red asterisks.

Figure 3

The Best Model Test Results

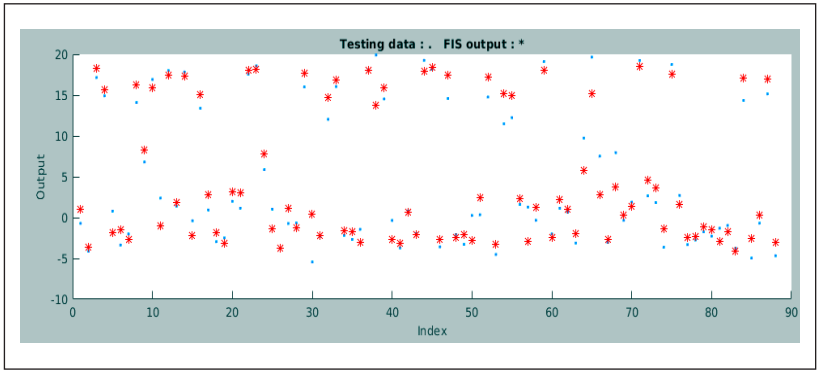

The correlation between m3 inputs (TaN, ΔTs) and the output (TaD) in the best model is illustrated in Figure 4. The smooth surface suggests a strong correlation between inputs and outputs.

Figure 4

The Best Model Surface Plot

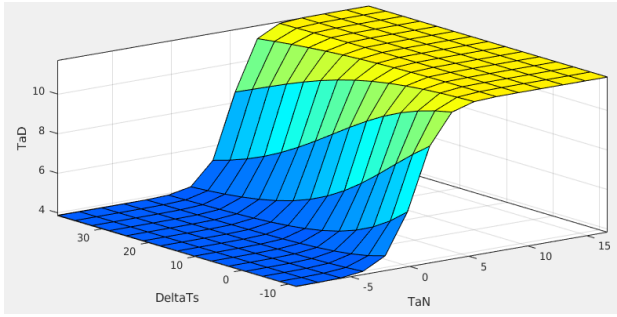

Models Ranking

To compare the various model and algorithm combinations in more detail, they were ranked from best performing (R1) to worst (R25) in Table 4. The following point can be concluded:

- Model-3 was the best-performing model combined with ANFIS.

Table 4

Models Ranking

Models	Inputs	ANFIS	Polynomial regression	Linear regression	LIBSVM	Simple regression tree
m1	TsN, TaN, TsD	R5	R4	R6	R13	R11
m2	TsN, TsD	R18	R17	R16	R23	R24
m3	TaN, ΔTs	R1	R3	R7	R9	R15
m4	ΔTs	R20	R19	R21	R22	R25
bm	TaN	R2	R8	R10	R12	R14

Model Reliability and Consistency Ranking

Table 5 summarizes the reliability and consistency rankings for each model. To determine model reliability, the mean ranking was utilized. Other than that, the range in the ranking (difference between best and worst ranks) was used to determine model consistency. A lower mean

ranking presents higher reliability, and a lower variation in rankings means higher consistency.

Here, m3 is the best in reliability ranking, followed by m1. The basic assumption of m3 is that taking TaN as the baseline and adding ΔTs (a proxy for solar radiation) to predict TaD can be accepted as a valid assumption in the desert zone. The presence of TaN in both good models highlights its importance as a baseline for predicting TaD. In contrast, the presence of TsN, TsD, and ΔTs in bad models highlights the insufficiency of Ts alone as a baseline for TaD estimation. Hence, the differences in consistency ranking reflect the differences between different input variables.

- Model-2 and Model-4 did not perform well in the desert zone. However, their consistency and reliability should be seen in the context of RMSE results in Table 3.
- The benchmark model with an average RMSE across all algorithms of 2.28783 performed well, proving the point that this one input and one output model works well in the desert zone and highlights the strong relationship between TaN and TaD.

Table 5

Models Reliability and Consistency Ranking

Model	Ranking average	Reliability ranking	Ranking variation	Consistency ranking
m1	7.8	2	9	3
m2	19.6	4	8	2
m3	7	1	14	5
m4	21.4	5	6	1
bm	9.2	3	12	4

Algorithm reliability and consistency ranking

The same concepts were applied to analyze each algorithm's reliability and consistency rankings in Table 6. ANFIS came up as the best algorithm in reliability ranking across all models, followed

by polynomial regression and Linear regression algorithms. Note that SVM is the most consistent but with poor results. The differences in consistency ranking should be referred to as differences between algorithms and models. Thus, the most reliable algorithms are not the most consistent in performance.

Table 6

Algorithms Reliability and Consistency Ranking

Algorithm	Ranking average	Reliability ranking	Ranking variation	Consistency ranking
ANFIS	9.2	1	19	5
Polynomial regression	10.2	2	16	4
Linear regression	12	3	15	3
SVM	15.8	4	13	1
Simple regression tree	17.8	5	14	2

Performance Evaluation

The performance of novel models was compared with the benchmark model. Overall, the novel models outperformed the benchmark model:

- 75% (three out of four models) are better in the consistency comparison
- 50% (two out of four models) are better in the reliability comparison

DISCUSSION

The desert zone surface consists of bare rock and sand with minimal protective vegetation. The intense solar radiation at high elevations during the day heats the surface, eventually influencing the Ta above the surface, creating some coupling between the two variables. The same strong coupling can be observed during the night, during which the absence of solar radiation cools the surface and, eventually, the air above. However, there is a big difference between the rock and air in terms of heat conductivity, leading to differential responses regarding heating/cooling. The surface is much more responsive than the air since the low atmospheric pressure (~500mb) at the top of the mountain: 5800m) makes conduction and convection relatively inefficient. Thus, Ta at 2m has a much-dampened response to energy

balance in comparison to the surface. This leads to different coupling patterns between Ta and Ts in the desert. Naturally, the Ta lags somewhat behind the Ts.

Three coupling areas can be identified on the surface plot (Figure 4). The flat blue surface at the bottom, the flat yellow surface at the top, and the mixed color surface at the middle. These surfaces are possibly related to night (blue), day (yellow), and the short transition periods of dawn and dusk (mixed). The blue and yellow surfaces represent areas of high coupling, whereas the middle surface represents an unstable regime between Ta and Ts.

In Figure 3, two groups of data points can clearly be identified, one with high temperatures (well above freezing) and one with much lower temperatures (below or around freezing). It is unusual for temperatures to be in between these two groups. This binary result is intriguing, but the exact cause requires further research since many factors could cause this. For example, the presence or absence of solar radiation is a critical control in the high-elevation desert environment, and any binary effect will likely result from this. This could, in turn, be related to conditions of cloud/no cloud, shade/no shade, station location (north-east slope aspect vs. southwest slope aspect), day/night, snow cover/no snow cover on the surface (which influences whether it can heat up or not) or some combination of all these.

There are five stations in the desert zone that receive a contrasting amount of solar radiation based on their location. Further research should focus on individual stations to investigate the impact of the location on model performance. Other than that, additional work will be required to transfer our findings to other environments on the mountain and elsewhere.

Our analysis has used the commonly used RMSE to evaluate model performance, and this approach is widely accepted. However, there are additional metrics that could be investigated, including the Akaike Information Criterion (AIC) and Bayesian Information Criterion (BIC).

CONCLUSION

Although the research confirms the reliability of ML algorithms (especially ANFIS) to estimate Ta from the satellite-measured Ts in

a high-elevation desert environment (>4500m) with few measured climate variables, the lack of enough coupling between Ta and Ts in this zone prevents the sole use of Ts as the only input. As a consequence, the Ta of the night still plays an important role. It should be utilized as input to get higher accuracy models, highlighting the need for increased weather station measurements in this zone. The results could apply to other desert areas, but further research is required to apply this approach to other areas and land-cover types on the mountain and further afield.

ACKNOWLEDGMENT

This research received no specific grant from any funding agency in the public, commercial, or not-for-profit sectors.

REFERENCES

Benali, A., Carvalho, A. C., Nunes, J. P., Carvalhais, N., & Santos, A. (2012). Estimating air surface temperature in Portugal using MODIS LST data. *Remote Sensing of Environment, 124*, 108–121. https://doi.org/10.1016/j.rse.2012.04.024

Bonissone, P. (n.d.). Adaptive Neural Fuzzy Inference Systems (ANFIS): Analysis and Applications. https://www.researchgate.net/profile/Alireza-Soloukdar/post/What-references-do-you-recommend-me-to-learn-ANFIS-for-forecasting-of-Organizational-systems-in-filed-of-Management/attachment/59d629f9c49f478072e9c800/AS %3A272527505059840%401441987028751/download/anfis.rpi04.pdf

Brieman, L., Friedman, J. H., Olshen, R. A., & Stone, C. J. (1984). Classification and regression trees. Wadsworth Inc, 67.

Colombi, A., De Michele, C., Pepe, M., Rampini, A., & Michele, C. D. (2007). Estimation of daily mean air temperature from MODIS LST in Alpine areas. *EARSeL eProceedings, 6*(1), 38–46.

Cortes, C., & Vapnik, V. (1995). Support-vector networks. *Machine Learning, 20*(3), 273–297. https://doi.org/10.1007/BF00994018

Hayati, M., & Mohebi, Z. (2007). Application of artificial neural networks for temperature forecasting. *World Academy of Science, Engineering and Technology, 28*(2), 275–279.

Hachem, S., Duguay, C., & Allard, M. (2012). Comparison of MODIS-derived land surface temperatures with ground surface and air

temperature measurements in continuous permafrost terrain. *The Cryosphere, 6*(1), 51–69. https://doi.org/10.5194/tc-6-51-2012

Hemp, A. (2009). Climate change and its impact on the forests of Kilimanjaro. *African Journal of Ecology, 47*, 3–10. https://doi.org/10.1111/j.1365-2028.2008.01043.x

Hemp, A. (2005). Climate change-driven forest fires marginalize the impact of ice cap wasting on Kilimanjaro. *Global Change Biology, 11*(7), 1013–1023. https://doi.org/10.1111/j.1365-2486.2005.00968.x

Jang, J.-D., Viau, A., & Anctil, F. (2004). Neural network estimation of air temperatures from AVHRR data. *International Journal of Remote Sensing, 25*(21), 4541–4554. https://doi.org/10.1080/01431160310001657533

Jang, J.-S. (1993). ANFIS: adaptive-network-based fuzzy inference system. *IEEE Transactions on Systems, Man, and Cybernetics, 23*(3), 665–685. doi: 10.1109/21.256541

Kumari, K. A., Boiroju, N. K., Ganesh, T., & Reddy, P. R. (2012). Forecasting surface air temperature using neural networks. *International Journal of Mathematics and Computer Applications Research, 3*, 65–78.

Kumar, P. (2012). Minimum weekly temperature forecasting using ANFIS. *Computer Engineering and Intelligent Systems, 3*(5), 1–6.

Knime Analytics Platform version 4.3.4 (4.3.4). (2020). [Computer software]. KNIME AG.

Lin, C.-J., & Chang, C. (2001). LIBSVM: a library for support vector machines, 2001. Software Available at 10(1961189.1961199).

MATLAB version R2020a. (2020). The Mathworks, Inc.

Mölg, T., Hardy, D. R., & Kaser, G. (2003). Solar-radiation-maintained glacier recession on Kilimanjaro drawn from combined ice-radiation geometry modeling. *Journal of Geophysical Research: Atmospheres, 10,* 4731.

Mote, P. W., & Kaser, G. (2007). The shrinking glaciers of Kilimanjaro: Can global warming be blamed? The Kibo ice cap, a" poster child" of global climate change, is being starved of snowfall and depleted by solar radiation. *American Scientist, 95*(4), 318–325. https://doi.org/10.1511/2007.66.318

Moninger, W. R., Davis, J., Dyer, R., Kittredge, R., McArthur, R., Murphy, A. H., & Racer, I. R. (1987). Summary of the first conference on Artificial Intelligence Research in Environmental

Sciences (AIRIES). *Bulletin of the American Meteorological Society, 68*(7), 793–800. http://www.jstor.org/stable/26225427

McCann, D. W. (1992). A neural network short-term forecast of significant thunderstorms. *Weather and Forecasting, 7*(3), 525–534. https://doi.org/10.1175/1520-0434(1992)007%3C0525:ANNSTF%3E2.0.CO;2

Neter, J., Kutner, M., Wasserman, W., & Nachtsheim, C. J. (1996). *Applied linear statistical models*, 4th edition. McGraw-Hill.

Palazzi, E., Mortarini, L., Terzago, S., & Von Hardenberg, J. (2019). Elevation-dependent warming in global climate model simulations at high spatial resolution. *Climate Dynamics, 52*(5–6), 2685–2702. https://doi.org/10.1007/s00382-018-4287-z

Pepin, N., Deng, H., Zhang, H., Zhang, F., Kang, S., & Yao, T. (2019). An examination of temperature trends at high elevations across the Tibetan Plateau: The use of MODIS LST to understand patterns of elevation-dependent warming. *Journal of Geophysical Research: Atmospheres, 124*(11), 5738-5756. https://doi.org/10.1029/2018JD029798

Pepin, N., Maeda, E. E., & Williams, R. (2016). Use of remotely sensed land surface temperature as a proxy for air temperatures at high elevations: Findings from a 5000 m elevational transect across Kilimanjaro. *Journal of Geophysical Research: Atmospheres, 121*(17), 9998–10. https://doi.org/10.1002/2016JD025497

Pepin, N. C. (2004). Meteorological data for 22 sites across Kilimanjaro. University of Portsmouth.

Potter, C., & Coppernoll-Houston, D. (2019). Controls on land surface temperature in deserts of Southern California derived from MODIS satellite time series analysis, 2000 to 2018. *Climate, 7*(2), 32. https://doi.org/10.3390/cli7020032

Shen, S., & Leptoukh, G. G. (2011). Estimation of surface air temperature over central and eastern Eurasia from MODIS land surface temperature. *Environmental Research Letters, 6*(4), 045206. http://dx.doi.org/10.1088/1748-9326/6/4/045206

Schizas, C. N., Michaelides, S., Pattichis, C. S., & Livesay, R. (1991). Artificial neural networks in forecasting minimum temperature (weather). *1991 Second International Conference on Artificial Neural Networks,* 112–114.

Shehzadex. (2021, 27 November). *Support vector machine.png.* https://commons.wikimedia.org/wiki/File:Kernel_yontemi_ile_veriyi_daha_fazla_dimensiyonlu_uzaya_tasima_islemi.png

Thompson, L. G., Mosley-Thompson, E., Davis, M. E., Henderson, K. A., Brecher, H. H., Zagorodnov, V. S., et al. (2002). Kilimanjaro ice core records: Evidence of Holocene climate change in tropical Africa. *Science, 298*(5593), 589–593. https://doi.org/10.1126/science.1073198

Urban, M., Eberle, J., Hüttich, C., Schmullius, C., & Herold, M. (2013). Comparison of satellite-derived land surface temperature and air temperature from meteorological stations on the pan-Arctic Scale. *Remote Sensing, 5*(5), 2348–2367. https://doi.org/10.3390/rs5052348

Vancutsem, C., Ceccato, P., Dinku, T., & Connor, S. J. (2010). Evaluation of MODIS land surface temperature data to estimate air temperature in different ecosystems over Africa. *Remote Sensing of Environment, 114*(2), 449–465. https://doi.org/10.1016/j.rse.2009.10.002

Xu, Y., Knudby, A., Shen, Y., & Liu, Y. (2018). Mapping monthly air temperature in the Tibetan Plateau from MODIS data based on machine learning methods. *IEEE Journal of Selected Topics in Applied Earth Observations and Remote Sensing, 11*(2), 345–354. doi: 10.1109/JSTARS.2017.2787191

Zhao, D., Zhang, W., & Shijin, X. (2007). A neural network algorithm to retrieve near surface air temperature from lands at ETM+ imagery over the Hanjiang River Basin, China. *2007 IEEE International Geoscience and Remote Sensing Symposium,* 1705–1708.

Zhou, C., & Wang, K. (2016). Land surface temperature over global deserts: Means, variability, and trends. *Journal of Geophysical Research: Atmospheres, 121*(24), 14–344. https://doi.org/10.1002/2016JD025410